metals

MDPI

Article

Nanoscale Twinned Ti-44Al-4Nb-1.5Mo-0.007Y Alloy Promoted by High Temperature Compression with High Strain Rate

Wenqi Guo, Haitao Jiang *, Shiwei Tian and Guihua Zhang

Engineering Research Institute, University of Science and Technology Beijing, Beijing 100083, China; guowenqi@ustb.edu.cn (W.G.); tswustb@sina.com (S.T.); zgh2004yall.com@126.com (G.Z.)

* Correspondence: jianght@ustb.edu.cn; Tel.: +86-135-2091-7917

Received: 27 May 2018; Accepted: 2 August 2018; Published: 7 August 2018

Abstract: In order to investigate the dynamic mechanical behavior of TiAl alloys and promote their application in the aerospace industry, uniaxial compression of Ti-44Al-4Nb-1.5Mo-0.007Y (at %) alloy was conducted at a temperature range from 25 to 400 °C with a strain rate of 2000 s^{-1}. Twinning is found to be the dominating deformation mechanism of the γ phase at all temperatures, and the addition of Nb and Mo has a chemical impact on the alloy and reduces the stacking fault energy of the γ phase. The decreased stacking fault energy increases the twinnability; thus, the deformation is dominated by twinning, which increases the dynamic strength of the alloy. With the temperature increasing from 25 to 400 °C, the average spacing of twins in the γ phase increases from 32.4 ± 2.9 to 88.1 ± 9.2 nm. The increased temperature impedes the continuous movement of partial dislocations and finally results in an increased twin spacing in the γ phase.

Keywords: TiAl alloy; high strain rate; mechanical property; deformation mechanism; twinning

1. Introduction

Titanium aluminum (TiAl) alloys are considered to be one of the most promising candidates for high temperature applications in the aerospace industry because of their high strength, low density and excellent creep properties [1–3]. For example, compared to nickel-based superalloys, TiAl alloys are ~35% lighter and exhibit great potential in the temperature range of 600–900 °C, which is the working range for the outer blades of turbine engines [4,5].

Conventional TiAl alloys (for example, Ti-48Al-2Cr-2Nb alloy), consisting of the γ phase and α_2 phase, have drawbacks such as low ductility (elongation is less than 5%) at room temperature and poor hot workability [6,7]. These disadvantages of TiAl alloys can be improved significantly by thermo-mechanical processing, such as hot rolling, hot forging, and hot extrusion [8], which also reduces the number of voids and refines grain sizes. The deformation mechanisms of thermally processed TiAl alloys have been systematically investigated in the literature [9]. The γ phase deforms mostly by dislocation slipping during high temperature treatments [10,11], discontinuous dynamic recrystallization [11], as well as phase transformation [12]. However, the hot workability of conventional (γ + α_2) TiAl alloys is poor, such that the material fractures during the forming process, thus largely restricting their application. In order to improve the mechanical properties as well as the hot workability of TiAl alloys, TNM alloys (also called β phase containing TiAl alloys) have been developed in recent years. In addition to the γ and α_2 phases, a disordered β phase exists in TNM alloys at a temperature range from 1100 to 1300 °C, which is mainly stabilized by Nb and other minor elements such as Mo, Cr, Y, etc. [13], and effectively improves the hot workability and plasticity.

The γ phase in traditional TiAl alloys can be deformed by twinning, which is an effective way to improve their mechanical properties [14]. With the modifying alloying elements added to TNM alloys,

the stacking fault energy of the γ phase is changed and the formation of twins is further promoted [15]. However, the major deformation mechanisms of TNM alloys under low strain rate conditions are still under debate, which include dislocation movement [16,17] and twinning [16–18], while the bulging of grain boundaries [18] and dynamic recrystallization [16] also contribute to the overall plasticity.

Except for mechanical properties under low strain rate conditions, the safety design of engines also requires that TNM alloys are stable under high strain rate conditions, such as dynamic impact caused by foreign objects—such as birds—that may collide against a turbine blade in an aircraft [19]. Thus, it is necessary to investigate the mechanical behavior of TiAl alloys under a high strain rate. Y.J. Hao et al. [20] investigated the dynamic mechanical behavior of Ti-47Al-2Cr-2Nb (at %) alloys and showed that the yield strength of the alloy is consistently 750 MPa in the temperature range of 15–500 °C. S.A. Maloy et al. [21] studied the compressive deformation behavior of T-48Al-2Nb-2Cr (at %) at strain rates of 0.001 s^{-1} and 2000 s^{-1}. Results show that deformation occurs in γ-TiAl by means of {111}<112] twinning and 1/2<110] slip. X. Zan et al. [22] investigated the dynamic deformation mechanisms of Ti-47Al-2Nb-2Cr (at %) alloy and concluded that deformation twins are common in equiaxed grains but that no twins are found in lamellar structures. However, most of the corresponding studies have been focused on conventional TiAl alloys, while the dynamic behavior of TNM is hardly known. As TNM alloys have good hot workability and show good application potential in engines, it is important to investigate their deformation mechanisms under high strain rate and high temperature.

The present paper aims at investigating the mechanical properties and deformation mechanisms of TNM alloys at temperatures of 25 °C, 200 °C and 400 °C with a high strain rate using a split Hopkinson pressure bar (SHPB). The dynamic deformation mechanisms of the TNM alloy are elucidated, and the twinning behavior of the γ phase is discussed.

2. Materials and Methods

A TNM alloy with a Ti-44Al-4Nb-1.5Mo-0.007Y (at %) alloy was prepared by induction skull melting. After solidification it was held at 1200 °C for 2 h under a pressure of 150 MPa, which was followed by cooling at a speed of 20 °C/min to room temperature. X-ray diffraction (XRD, Bruker Karlsruhe, Germany) was used to identify the phases of the TNM alloy. The target material used was Cu and the 2θ range was from 10 to 100°.

Uniaxial dynamic compressive experiments were performed at temperatures of 25 °C, 200 °C and 400 °C at the strain rate of 2000 s^{-1} using a SHPB system [23] comprised of a striker bar, incident bar, and transmitted bar, and the schematic diagram is shown in Figure 1a. The diameter of each bar was 14.5 mm. The length of the striker bar was 200 mm. The length of the incident bar and the transmitted bar was 700 mm. All compression tests were conducted on cylindrical specimens with 5 mm diameter and 5 mm height. Prior to the dynamic compression testing, these cylindrical samples were heated in a small tubular furnace and held at the testing temperature for 10 min [20]. Figure 1b,c are the pictures of the SHPB system and the heating device. During the test, the heating device is placed between incident bar and transmitted bar, as shown in the red rectangle in Figure 1b. To ensure the reliability of the experimental data, all tested specimens were subjected to the same impact velocity of the striker bar so as to obtain the same loading condition. In addition, at least three samples were tested under each testing condition to make sure that the experimental data were reproducible to within the limits of the equipment.

The deformed specimens were sectioned parallel to the compression axis using Electrical discharge machining (Xiangyonghui, Beijing, China) for microstructural analysis. Microstructures before and after dynamic compression were examined by Quanta 450FEG field-emission scanning electron microscopy (SEM, F20 FEI, Hillsboro, OR, USA). Electron back scattered diffraction (EBSD) observations were performed on a ZEISS ULTRA 55 (ZEISS, Jena, Germany). A JEOL JEM 2100 transmission electron microscopy (TEM, JEOL, Tokyo, Japan) with an acceleration voltage of 200 kV was employed to analyze the deformation mechanism of the TNM alloy. The specimens for TEM were prepared using twin-jet electropolishing method.

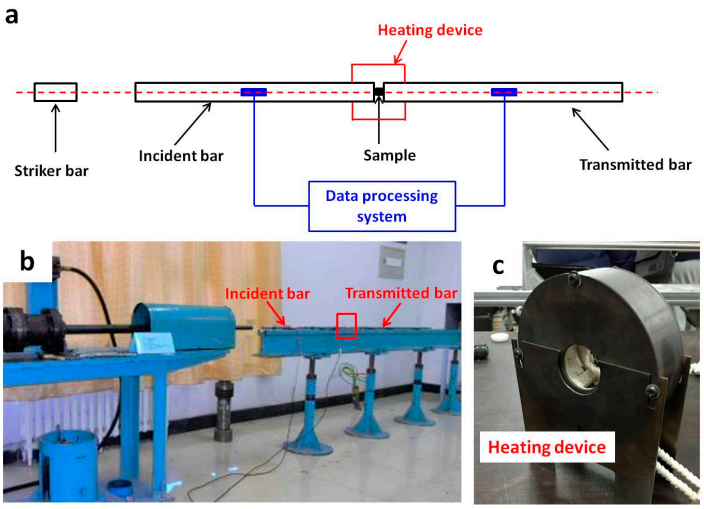

Figure 1. (**a**) Schematic diagram of the split Hopkinson pressure bar (SHPB) system; (**b**) picture of the SHPB system; (**c**) picture of the heating device.

3. Results

Figure 2a shows the XRD measurement of the heat-treated TNM alloy, in which γ-TiAl, α_2-Ti_3Al and B2 are detected. An SEM image with an EBSD image overlay is shown in Figure 2b. The TNM alloy is mainly composed of a γ/α_2 lamellar colony with an average size of ~50 μm and equiaxed γ grains, as well as the B2 phase. EBSD results show that the volume fractions of γ, α_2 and B2 phase are 82.5%, 12.7% and 4.8%, respectively. Figure 2c,d show TEM images of the heat-treated TNM alloy. The average inter-lamellae spacing of γ/α_2 lamellae is about 300 nm, and a B2 grain with a size of 500 nm is also observed. The inset in Figure 2d is the corresponding selected area electron diffraction (SAED), showing the CsCl structure of the B2 grain.

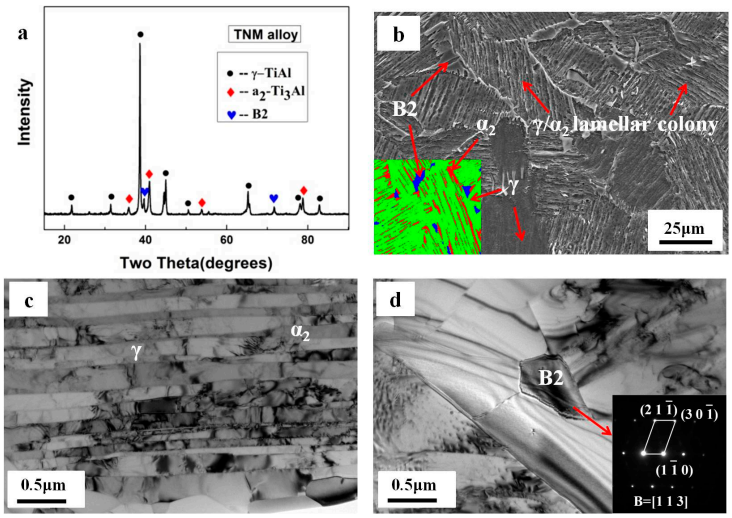

Figure 2. (**a**) XRD spectra showing that γ-TiAl, B2 and α_2-Ti_3Al phases exists in TNM alloy; (**b**) SEM image and EBSD image showing the γ phase (green color), α_2 phase (red color) and B2 phase (blue color); (**c**,**d**) TEM images and corresponding selected area electron diffraction (SAED) pattern showing the γ/α_2 lamellae and B2 phase.

Figure 3a shows the true stress-strain curves of the TNM alloy under dynamic compression at different temperatures. The dynamic yield strength of the TNM alloy decreases as testing temperature rises: 1320 ± 35 MPa at room temperature (25 °C), 1230 ± 30 MPa at 200 °C and 1120 ± 33 MPa at

400 °C. All of the dynamic yield strengths of the tested TNM alloy in this study are much higher than that of γ-TiAl alloys (~750 MPa at temperature range from 25 °C to 500 °C) [20]. One of the reasons for the difference in the strength of these alloys could be the hard B2 phase, which does not exist in the conventional TiAl alloys. However, the content of the B2 phase in TNM alloys is only 4.8%; thus, the increased yield strength also comes from a strengthening of the γ phase, possibly by deformation twins. Figure 3b–d show SEM micrographs of the TNM alloy deformed at 25 °C, 200 °C, and 400 °C, respectively. Since the true strain of TNM alloy under three deformation temperatures is similar and small (~0.12) after dynamic compression, the deformation of lamellae colonies in TNM alloy is slight, as shown in Figure 3b–d.

In order to investigate the deformation mechanism of the γ phase at different temperatures, the deformed microstructures were observed by TEM. The deformation of the γ-TiAl phase is usually controlled by {111}1/2<1 −1 0] full dislocation and {111}1/6<1 1 −2> twinning systems [24]. Figure 4a1 shows the TEM micrograph of the TNM alloy deformed at 25 °C. Deformation twins are formed in γ-TiAl lamellae, as indicated by the red arrows. An SAED pattern of the twins is shown in Figure 4a2. The average space between the twins in the γ phase is measured to be 32.4 ± 2.9 nm at 25 °C. Figure 4b1,c1 show TEM micrographs of the TNM alloy deformed at 200 °C and 400 °C respectively. Similarly, deformation twins are also observed in local region of γ-TiAl lamellar, and SAED patterns of the twins are shown in Figure 4b2,c2. Therefore, twinning is an important deformation mechanism for the γ phase in the TNM alloy between 25 °C and 400 °C.

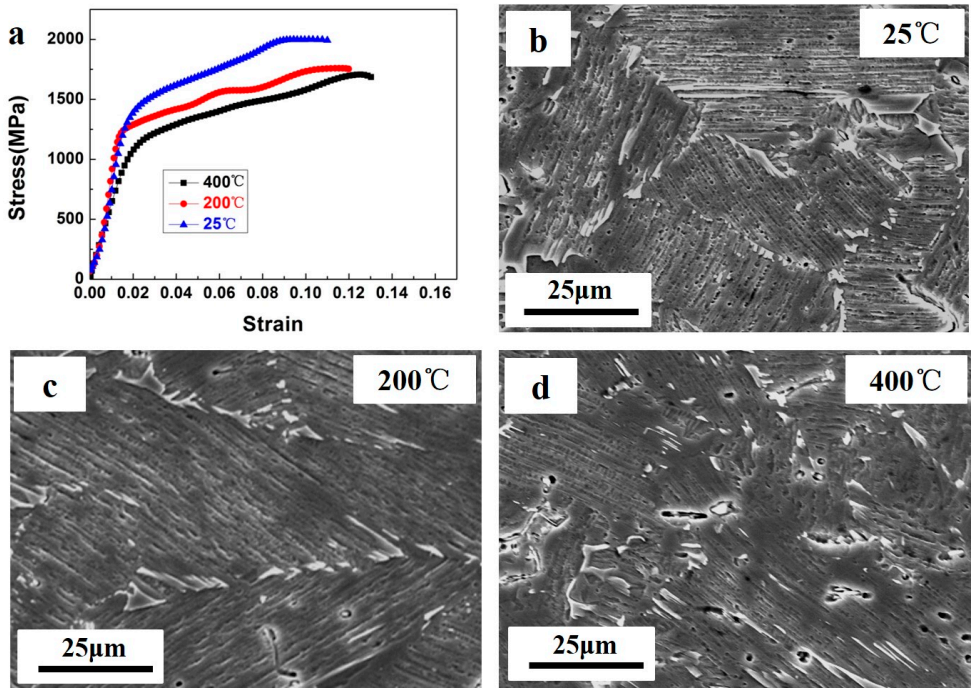

Figure 3. (**a**) The true stress-strain curves of TNM alloy under dynamic compression at different temperatures. SEM images of the deformed TNM alloy with a strain rate of 2000 s^{-1} at (**b**) 25 °C; (**c**) 200 °C; (**d**) 400 °C.

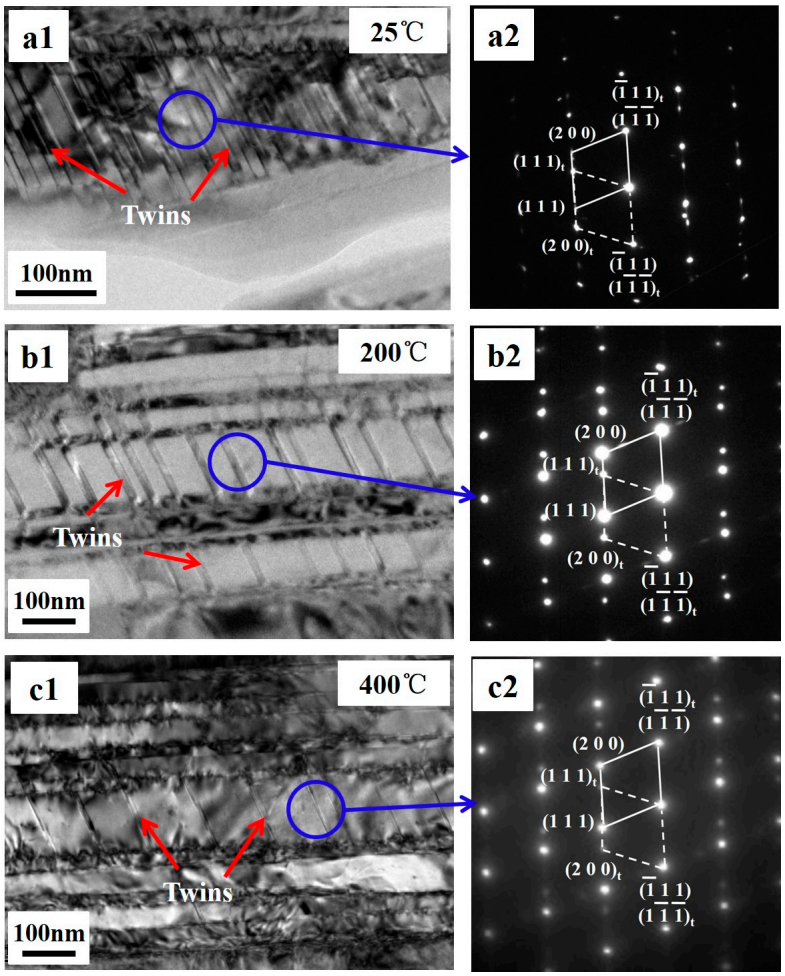

Figure 4. TEM micrographs and SAED of TNM alloy deformed at (**a1**,**a2**) 25 °C showing twins; (**b1**,**b2**) 200 °C showing twins; (**c1**,**c2**) 400 °C showing twins.

4. Discussion

The difference between the γ phases of TiAl and TNM could be explained by the additional elements Nb and Mo [15], which change the stacking fault energy. Additive elements such as Nb, Mo, Cr, Hf, and Ta relax the atomic position and lead to a decrease of the stacking fault energy by 20–40%. Among these elements, Nb and Mo have a significant influence on stacking fault energy. The superlattice intrinsic stacking fault of γ-TiAl drops by 36% after adding the Mo element, while the Nb element causes a 30% drop of the superlattice intrinsic stacking fault [25]. When the stacking fault energy is decreased, twins are easily formed. Thus, the twins in γ phase of current TNM alloy are considered to be promoted by the decreased stacking fault energy.

The average spacing of twins in the γ phase at 200 °C and 400 °C is 63.5 ± 6.2 nm and 88.1 ± 9.2 nm, increasing 95.9% and 171.9% compared to that at 25 °C. Therefore, as the temperature increases, the average spacing of twins shows a sharply increasing tendency, which means that twin formation is easier at lower temperatures. This phenomenon can also be explained by the increasing stacking fault energy as temperature increases, leading to impeded continuous movement of partial dislocations and finally resulting in an increased twin spacing.

The evolution of twins involves nucleation, propagation and thickening. In the γ-TiAl phase, twinning relies on the motion of {111}1/6<1 1 −2] Shockley partial dislocations. The twin planes are {111} close-packed planes, and the twinning direction is <1 1 −2]. Figure 5a show the high resolution TEM micrograph of twins observed in γ-TiAl lamellae of the TNM alloy. Nano-twin boundaries are

observed and marked by the dotted red line. The inset in Figure 5a shows the fast Fourier transform (FFT) of the region in the red circle, confirming the existence of the nano-twins. Under the strain rate of 2000 s^{-1}, the TNM alloy has a high twinnablity; nano-twins are prone to be activated at room temperature, and these deformation twins play an important role in increasing the dynamic strength of the TNM alloy. Based on our experimental results in Figure 5a, a schematic model showing the evolution of the twinning of the γ phase in the TNM alloy is built, as shown in Figure 5b1–b3. Figure 5b1 shows the γ phase before deformation. Under the dynamic compression condition, a stacking fault is first nucleated in the matrix under the motion of Shockley partial dislocations, as shown in Figure 5b2. After formation of the first layer, a second Shockley partial dislocation glides on adjacent planes. As Shockley partial dislocations continue to glide, the number of layers increases, resulting in the thickening and boundary migration of the twin, as shown in Figure 5b3.

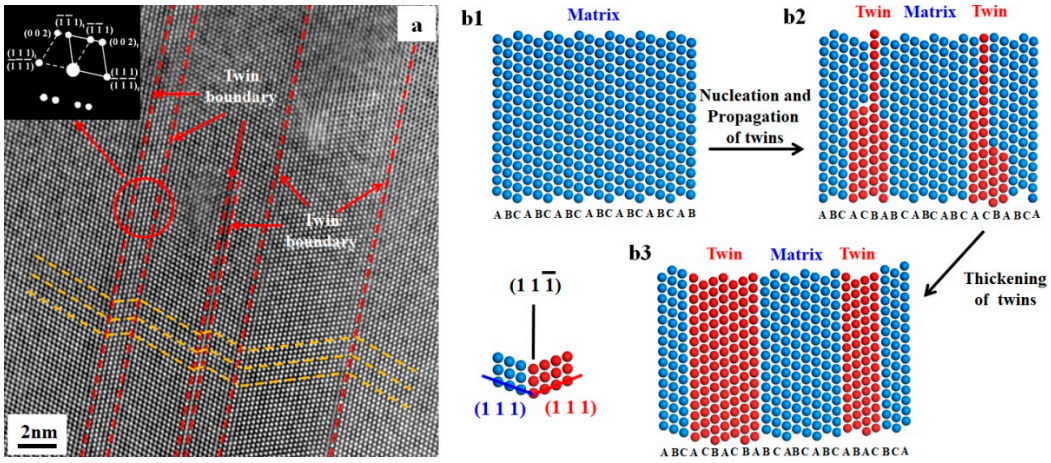

Figure 5. (**a**) High resolution TEM micrographs and a fast Fourier transform pattern of twins observed in γ-TiAl lamellae of TNM alloy deformed at 25 °C; a schematic model showing twinning evolution of the γ-TiAl phase in the TNM alloy; (**b1**) original state of the material; (**b2**) nucleation and propagation of twins; (**b3**) the thickening and boundary migration of twins.

5. Conclusions

In summary, twinning is the dominant deformation mechanism of the γ phase in Ti-44Al-4Nb-1.5Mo-0.007Y (at %) alloy at the strain rate of 2000 s^{-1} at temperature range of 25 °C to 400 °C, which is different from the conventional TiAl alloy. The addition of Nb and Mo has a chemical impact on γ phase and reduces the stacking fault energy. The decreased stacking fault energy increases the twinnability; thus the deformation is dominated by twinning, which increases the dynamic strength of the alloy. With the temperature increasing from 25 to 400 °C, the average spacing of twins in the γ phase increases from 32.4 ± 2.9 to 88.1 ± 9.2 nm. The increased temperature makes twinning more difficult and results in an increased twin spacing in the γ phase.

Author Contributions: W.G., H.J., S.T. and G.Z. designed and conducted the experiments; W.G. and H.J. performed the experiments; S.T. analyzed the data; H.J., and G.Z. contributed materials/analysis tools; W.G. wrote the paper.

Funding: This research is funded by the Fundamental Research Funds for the Central Universities (No. FRF-TP-17-006A1) and China Postdoctoral Science Foundation Grant (No. 2017M610762).

Conflicts of Interest: The authors declare no conflicts of interest.

References

1. Wei, D.X.; Koizumi, Y.; Nagasako, M.; Chiba, A. Refinement of lamellar structures in Ti-Al alloy. *Acta Mater.* **2017**, *125*, 81–97. [CrossRef]
2. Bartels, A.; Clemens, H.; Dehm, G.; Lach, E.; Schillinger, W. Strain Rate Dependence of the Deformation Mechanisms in a Fully Lamellar γ-TiAl-Based Alloy. *Zeitschrift für Metallkunde* **2002**, *93*, 180–185. [CrossRef]
3. Erdely, P.; Staron, P.; Maawad, E. Effect of hot rolling and primary annealing on the microstructure and texture of a β-stabilised γ-TiAl based alloy. *Acta Mater.* **2017**, *126*, 145–153. [CrossRef]
4. Wang, Q.; Ding, H.S.; Zhang, H. Influence of Mn addition on the microstructure and mechanical properties of a directionally solidified γ-TiAl alloy. *Mater. Charact.* **2018**, *137*, 133–141. [CrossRef]
5. Vajpai, S.K.; Ameyama, K. A novel powder metallurgy processing approach to prepare fine-grained Ti-rich TiAl-based alloys from pre-alloyed powders. *Intermetallics* **2013**, *42*, 146–155. [CrossRef]
6. Draper, S.L.; Krause, D.; Lerch, B. Development and evaluation of TiAl sheet structures for hypersonic applications. *Mater. Sci. Eng. A* **2007**, *464*, 330–342. [CrossRef]
7. Clemens, H.; Kestler, H. Processing and Applications of Intermetallic γ-TiAl-Based Alloys. *Adv. Eng. Mater.* **2000**, *2*, 551–570. [CrossRef]
8. Clemens, H.; Mayer, S. Design, Processing, Microstructure, Properties, and Applications of Advanced Intermetallic TiAl Alloys. *Adv. Eng. Mater.* **2013**, *15*, 191–215. [CrossRef]
9. Liang, X.; Liu, Y.; Li, H.; Gan, Z. An investigation on microstructural and mechanical properties of powder metallurgical TiAl alloy during hot pack-rolling. *Mater. Sci. Eng. A* **2014**, *619*, 265–273. [CrossRef]
10. Monchoux, J.P.; Luo, J.S.; Voisin, T. Deformation modes and size effect in near-γ TiAl alloys. *Mater. Sci. Eng. A* **2017**, *679*, 123–132. [CrossRef]
11. Cheng, L.; Li, J.S.; Xue, X.Y. Superplastic deformation mechanisms of high Nb containing TiAl alloy with (α_2 + γ) microstructure. *Intermetallics* **2016**, *75*, 62–71. [CrossRef]
12. Cao, G.H.; Russell, A.M.; Oertel, C.-G. Microstructural evolution of TiAl-based alloys deformed by high-pressure torsion. *Acta Mater.* **2015**, *98*, 103–112. [CrossRef]
13. Chen, G.L.; Zhang, L.C. Deformation mechanism at large strains in a high-Nb-containing TiAL at room temperature. *Mater. Sci. Eng. A* **2002**, *329*, 163–170. [CrossRef]
14. Rackel, M.W.; Stark, A.; Gabrisch, H. Orthorhombic phase formation in a Nb-rich γ-TiAl based alloy—An in situ synchrotron radiation investigation. *Acta Mater.* **2016**, *121*, 343–351. [CrossRef]
15. Jiang, H.T.; Tian, S.W.; Guo, W.Q. Hot deformation behavior and deformation mechanism of two TiAl-Mo alloys during hot compression. *Mater. Sci. Eng. A* **2018**, *719*, 104–111. [CrossRef]
16. Jiang, H.T.; Zeng, S.W.; Zhao, A.M. Hot deformation behavior of β phase containing γ-TiAl alloy. *Mater. Sci. Eng. A* **2016**, *661*, 160–167. [CrossRef]
17. Niu, H.Z.; Chen, Y.Y.; Xiao, S.L. High temperature deformation behaviors of Ti-45Al-2Nb-1.5V-1Mo-Y alloy. *Intermetallics* **2011**, *19*, 1767–1774. [CrossRef]
18. Wang, G.; Xu, L.; Tian, Y.X. Flow behavior and microstructure evolution of a P/M TiAl alloy during high temperature deformation. *Mater. Sci. Eng. A* **2011**, *528*, 6754–6763. [CrossRef]
19. Kothari, K.; Radhakrishnan, R.; Wereley, N.M. Advances in gamma titanium aluminides and their manufacturing techniques. *Prog. Aerosp. Sci.* **2012**, *55*, 1–16. [CrossRef]
20. Hao, Y.J.; Liu, J.X.; Li, J.C. Investigation on dynamic properties and failure mechanisms of Ti–47Al–2Cr–2Nb alloy under uniaxial dynamic compression at a temperature range of 288 K–773 K. *J. Alloys Compd.* **2015**, *649*, 122–127.
21. Maloy, S.A.; Gray, G.T., III. High strain rate deformation of Ti–48Al–2Nb–2Cr. *Acta Mater.* **1996**, *44*, 1741–1756. [CrossRef]
22. Zan, X.; Wang, Y.; Xia, Y.M. Strain rate effect on the tensile behavior of Duplex Ti–46.5Al–2Nb–2Cr intermetallics at elevated temperatures. *Mater. Sci. Eng. A* **2008**, *498*, 296–301. [CrossRef]
23. Wang, L.; Wang, Y.C.; Zhilyaev, A.P.; Korznikov, A.V.; Li, S.K.; Korznikova, E.; Langdon, T.G. Dynamic compressive behavior of ultrafine-grained pure Ti at elevated temperatures after processing by ECAP. *J. Mater. Sci.* **2014**, *49*, 6640–6647. [CrossRef]

24. Chen, G.; Peng, Y.B.; Zheng, G. Polysynthetic twinned TiAl single crystals for high-temperature applications. *Nat. Mater.* **2016**, *15*, 876–882. [CrossRef] [PubMed]
25. Dumitraschkewitz, P.; Clemens, H.; Mayer, S.; Holec, D. Impact of Alloying on Stacking Fault Energies in γ-TiAl. *Appl. Sci.* **2017**, *7*, 1193. [CrossRef]